Electron delocalization in bilayer graphene induced by an electric field

Mikito Koshino
Department of Physics, Tokyo Institute of Technology, Meguro-ku, Tokyo 152-8551, Japan
(Received 5 August 2008; published 9 October 2008)

Electronic localization is numerically studied in disordered bilayer graphene with an electric-field-induced energy gap. Bilayer graphene is a zero-gap semiconductor, in which an energy gap can be opened and controlled by an external electric field perpendicular to the layer plane. We found that, in the smooth disorder potential not mixing the states in different valleys (K and K' points), the gap opening causes a phase transition at which the electronic localization length diverges. We show that this can be interpreted as the integer quantum Hall transition at each single valley, even though the magnetic field is absent.

DOI: 10.1103/PhysRevB.78.155411 PACS number(s): 73.22.−f, 72.10.−d, 72.15.Rn, 73.43.−f

Since the experimental discovery of monatomic graphene,[1–3] the electronic properties of graphene-related materials have been extensively studied. The graphene bilayer, which is also experimentally available,[2,4,5] was shown to have a unique band structure distinct from monolayer, where the conduction and valence bands with quadratic dispersion touch at K and K' points in the Brillouin zone.[6] The transport properties of the bilayer graphene have been studied experimentally[4,7,8] and also extensively studied in theories.[9–13] The quantum correction to the conductivity, which is important in the low temperature, was studied for monolayer graphene[14,15] and for bilayer.[7,16] A unique property of bilayer graphene is that an electric field applied perpendicularly to the layers opens an energy gap between the electron and hole bands.[6,17–20] The transport property of the gapped bilayer graphene was also studied.[21] The electric-field-induced energy gap was observed in recent experiments.[5,22]

When the impurity potential is smooth compared to the atomic scale and the intervalley scattering is negligible, we can treat two valleys (around K or K') as independent subsystems. The sub-Hamiltonian within each valley generally has no time-reversal symmetry in itself since the time-reversal counterpart of the states at K exists at K'.[14,16] In bilayer graphene with a gap, interestingly, each sub-Hamiltonian has nonzero Hall conductivity even in zero magnetic field. The monolayer graphene can also have an energy gap and the corresponding Hall conductivity when the sublattice symmetry is broken,[23,24] while it cannot be controlled externally.[25]

The single-valley Hall conductivity can never be directly observed since it is exactly canceled by the contribution from the other valley. In this paper, however, we find that this quantity strongly influences the electron localization properties, and this may be observed in the longitudinal conductivity. We show that, when the system is under smooth random potential not mixing valleys, the perpendicular electric field causes a phase transition at which the localization length diverges. We find that this is interpreted as the quantum Hall transition at each single valley, where the single-valley Hall conductivity changes from one integer to another. To demonstrate this, we numerically calculate the localization length in disordered bilayer graphene with electric fields to actually show that the localization length diverges at a certain field amplitude. We then calculate the single-valley Hall conductivity and show that the delocalization is actually associated with the transition between different quantum Hall phases.

Bilayer graphene is composed of a pair of hexagonal networks of carbon atoms, which include A and B atoms on the bottom layer and A' and B' on the top. As shown in Fig. 1, both layers are arranged in the Bernal stacking, where A atoms are located directly below B' atoms.[6] The low-energy spectrum is given by the states around K and K' points in the Brillouin zone. Neighboring A and B' sites are coupled to create high-energy bands, and remaining A' and B sites form the low-energy bands touching at the zero energy. The effective low-energy Hamiltonian around K point reads[6]

$$\mathcal{H}_0^K = \begin{pmatrix} \Delta & \frac{\hbar^2}{2m^*}(k_x - ik_y)^2 \\ \frac{\hbar^2}{2m^*}(k_x + ik_y)^2 & -\Delta \end{pmatrix}, \qquad (1)$$

which operates on a wave function $(F_{A'}^K, F_B^K)$, where F_X^K represents the value of the envelope function of K point at site X. Here Δ and $-\Delta$ are the external electrostatic potential at the top and bottom layers, respectively, due to the applied electric field and m^* is the effective band mass defined by $m^* = \gamma_1/(2v^2)$, where γ_1 is the coupling parameter for the vertical bonds between A and B' atoms, and v is the velocity of the monolayer graphene.[6] We assume that Δ and vk are much smaller than γ_1 and neglect the terms more than the third order in Δ/γ_1 and vk/γ_1. The band structure of a real bilayer graphene is trigonally warped due to the extra coupling parameter between A' and B (Refs. 6 and 9) but is

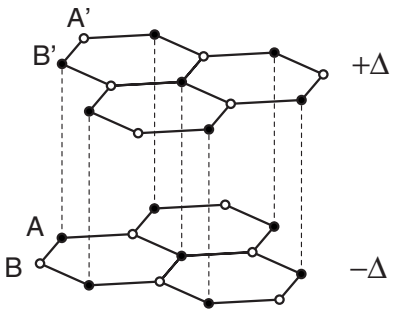

FIG. 1. Atomic structure of the bilayer graphene. $+\Delta$ and $-\Delta$ represent the potential of the top and bottom layers, respectively.

neglected here for simplicity. The eigenenergy of Eq. (1) is given by

$$\varepsilon_{\mathbf{k}s} = s\sqrt{\left(\frac{\hbar^2 k^2}{2m^*}\right)^2 + \Delta^2} \tag{2}$$

with $s=\pm$ and $k=\sqrt{k_x^2+k_y^2}$. The energy gap extends between $\varepsilon=\pm\Delta$. The effective Hamiltonian for K' can be obtained by exchanging k_x+ik_y and k_x-ik_y, giving the basically same spectrum. In the absence of Δ, the density of states (DOS) becomes constant, $\rho_0=m^*/(2\pi\hbar^2)$ per valley and per spin.

For the disorder potential, we assume that the length scale is much longer than the atomic scale and neglect the intervalley scattering. This should be valid as long as the phase-coherent time is smaller than the intervalley scattering time.[14,16] We also assume that the disorder length scale is shorter than the typical wavelength of $2\pi/k$ with k being the wave number from K or K' points, so as to be modeled as a short-ranged potential within the valley decoupled Hamiltonian. This is then expressed as[9]

$$V = \sum_i u_i \delta(\mathbf{r}-\mathbf{r}_i)\begin{pmatrix} 1 & 0 \\ 0 & 1 \end{pmatrix}. \tag{3}$$

We assume an equal amount of positive and negative scatterers $u_i=\pm u$ and a total density per unit area n_{imp}. At $\Delta=0$, the energy broadening $\Gamma=\hbar/(2\tau)$ becomes independent of the energy in the weak disorder limit and is expressed by[9]

$$\Gamma = \frac{\pi n_{\mathrm{imp}} u^2 \rho_0}{2}.$$

This will be used as the energy scale characterizing the disorder strength. We also introduce unit wave number k_0 as $\hbar^2 k_0^2/(2m^*)=\Gamma/2$ and unit length $\lambda_0=2\pi/k_0$.

The single-valley Hamiltonian with disordered potential $\mathcal{H}^K=\mathcal{H}_0^K+V$ belongs to the unitary symmetry class when Δ is nonzero. It becomes the orthogonal class only at $\Delta=0$ as we have the relation $\sigma_x\mathcal{H}^K\sigma_x=(\mathcal{H}^K)^*$ with the Pauli matrix σ_x. This is an effective time-reversal symmetry within a single valley and should be distinguished from the real time-reversal symmetry connecting K and K' which always exists at any values of Δ.

The single-valley Hamiltonian has a nonzero Hall conductivity when $\Delta\neq 0$. This is estimated by the Kubo formula

$$\sigma_{xy} = \frac{\hbar e^2}{iS}\sum_{\alpha,\beta}\frac{f(\varepsilon_\alpha)-f(\varepsilon_\beta)}{\varepsilon_\alpha-\varepsilon_\beta}\frac{\langle\alpha|v_x|\beta\rangle\langle\beta|v_y|\alpha\rangle}{\varepsilon_\alpha-\varepsilon_\beta+i\delta}, \tag{4}$$

where S is the area of the system, v_x and v_y are the velocity operators, δ is the positive infinitesimal, $f(\varepsilon)$ is the Fermi distribution function, and $|\alpha\rangle$ and ε_α describe the eigenstate and the eigenenergy of the system, respectively.

By applying this formula to the ideal K-point Hamiltonian $\mathcal{H}_0^K$ at zero temperature, we obtain

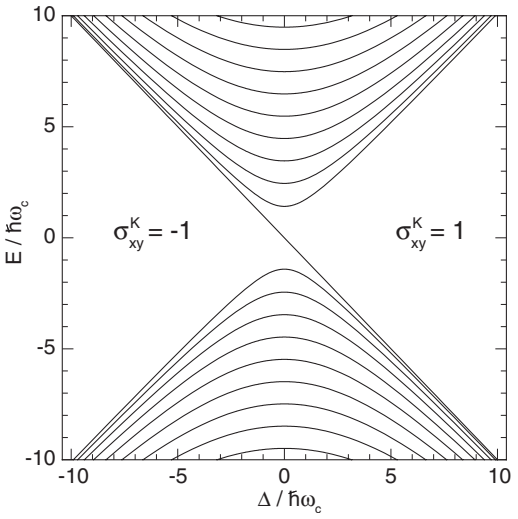

FIG. 2. Energy spectrum Eq. (6) plotted against Δ at K valley in the bilayer graphene with a uniform magnetic field.

$$\sigma_{xy}^K = \begin{cases} \dfrac{e^2}{h}\dfrac{\Delta}{|\varepsilon_F|} & |\varepsilon_F| > |\Delta| \\ \dfrac{e^2}{h}\mathrm{sgn}(\Delta) & |\varepsilon_F| < |\Delta| \end{cases} \tag{5}$$

with $\mathrm{sgn}(x)=x/|x|$. The result for K' point is given by $\sigma_{xy}^{K'}=-\sigma_{xy}^K$, so that the net Hall conductivity is exactly zero as it should. σ_{xy}^K at the energy gap is quantized into different values in the negative and positive Δ's. When ε_F is fixed to zero and Δ is continuously changed from negative to positive, we have the Hall conductivity change from $\sigma_{xy}^K=-e^2/h$ to e^2/h and from $\sigma_{xy}^{K'}=e^2/h$ to $-e^2/h$.

The jump of the Hall conductivity can be intuitively explained by the consideration of the energy spectrum in the magnetic field. In a uniform field B, the Landau-level energy at K is obtained by substituting $\mathbf{k}$ in Eq. (1) with $\mathbf{k}+e\mathbf{A}/\hbar$ with the vector potential $\mathbf{A}=(0,Bx)$.[6] This results in

$$\varepsilon_{s,n} = s\sqrt{(\hbar\omega_c)^2 n(n-1)+\Delta^2} \quad (n\geq 2),$$

$$\varepsilon_0 = \varepsilon_1 = -\Delta, \tag{6}$$

where $\omega_c=eB/m^*$ and $s=\pm$ represents the electron and hole bands. The energy spectrum is plotted as a function of Δ in Fig. 2. We have doubly degenerate Landau levels ε_0 and ε_1 at $E=-\Delta$, which move from the electron band down to the hole band as Δ increases. When the Fermi energy is fixed at $E_F=0$ and Δ is changed from negative to positive, those two Landau levels cross E_F and therefore give a change in σ_{xy}^K by $2e^2/h$, which is twice as large as a Hall conductivity quantum. It is important that this discontinuity in σ_{xy}^K is not dissolved in the limit of $B\to 0$, and it is actually consistent with the discussion above in zero magnetic field. For K' point, we have $\varepsilon_0=\varepsilon_1=+\Delta$, leading to the opposite sign of the Hall conductivity change.

Now we numerically calculate the electronic states in the disorder potential by exactly diagonalizing the Hamiltonian matrix. We consider a finite square system with $L\times L$ de-

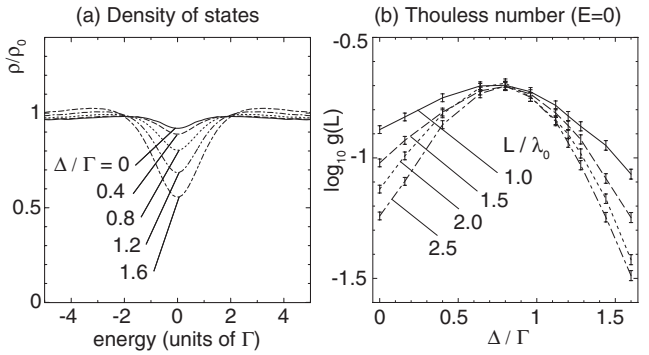

FIG. 3. (a) Density of states as a function of energy in bilayer graphene with several Δ's at fixed Γ. (b) Thouless number g at zero energy plotted against Δ.

scribed by the K point Hamiltonian $\mathcal{H}^K=\mathcal{H}_0^K+V$, imposing a boundary condition with phase factors $\exp(i\phi_x)$ and $\exp(i\phi_y)$ for x- and y-directions, respectively. To make the matrix finite, we introduce the k-space cutoff $k_c=6k_0$, which corresponds to $\varepsilon_c=18\Gamma$.

To investigate the localization property, we calculate the Thouless number g, which is the ratio of the shift ΔE of each energy level due to the change in the boundary condition to the level spacing $[L^2\rho]^{-1}$ with ρ being the density of states per unit area.[26] We estimate the energy shift by $\Delta E = \pi\langle|\partial^2 E(\phi)/\partial\phi^2|\rangle$, where $E(\phi)$ represents the eigenenergy as a function of the boundary phase $\phi=\phi_x$ with fixed ϕ_y and $\langle\ \rangle$ represents averaging over different levels in a small energy region around the energy ε in question. The localization length L_{loc} is estimated by fitting the results to $g(L) \propto \exp(-L/L_{\mathrm{loc}})$. When $g \ll 1$, g is approximately related to the longitudinal conductivity σ_{xx} by $\sigma_{xx} \sim (e^2/\hbar)g$.[26] We also calculate the Hall conductivity by substituting the eigenstates of the disordered system to the Kubo formula (4). For every quantity, we take an average over a number of samples with different configuration of the disorder potential and boundary phase factors ϕ_x, ϕ_y.

The absolute value of σ_{xy} generally depends on the k-space cutoff. This is because σ_{xy} can be expressed as the summation of the contribution from all the occupied states below the Fermi energy unlike σ_{xx} which only depends on the states at the Fermi energy. In the clean limit, the cutoff at $\varepsilon=\pm\varepsilon_c$ leads to overall shift of $\sigma_{xy}(\varepsilon)$ by a constant $(e^2/h)\Delta/\varepsilon_c$, which is the contribution from the missing states out of the cutoff. σ_{xy} in the disordered system has a similar shift which vanishes in the limit of $\varepsilon_c \to 0$. However, as long as ε_c is much larger than the energy broadening Γ, it hardly changes the function form of $\sigma_{xy}(\varepsilon)$ around $\varepsilon=0$ except for this small constant.

Figure 3(a) shows the DOS in disordered bilayer graphene with various Δ's at fixed Γ. The energy axis is scaled in units of Γ. As Δ increases, the DOS at the zero energy monotonically decreases as expected, while the disorder potential fills the energy gap with some states. In Fig. 3(b), we plot the Thouless number g at zero energy as a function of Δ for several system sizes. We naively expect that the conductivity at zero energy monotonically decreases in increasing Δ since the DOS becomes smaller, but this is not the case here. At

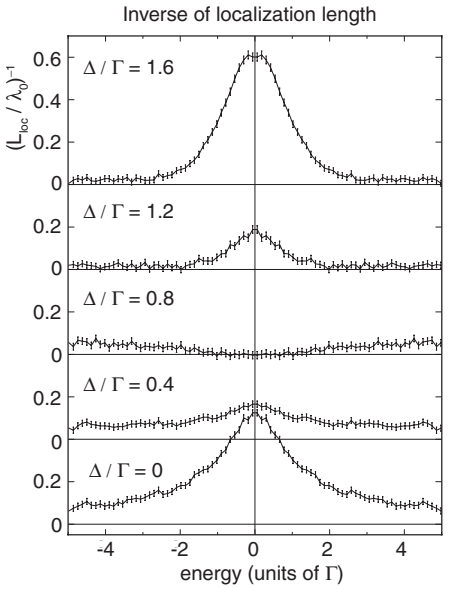

FIG. 4. Inverse of the localization as a function of energy in bilayer graphene with several Δ's.

every system size, g goes up first when Δ starts from 0 and then changes to decrease at $\Delta \sim 0.8\Gamma$. Significantly g becomes independent of the system size around the peak, while in other regions it drops exponentially as the system size increases. This suggests that the electronic state at zero energy is localized both in small and large Δ's but delocalized only at $\Delta \sim 0.8\Gamma$. We calculate g also for other energies and obtain the localization length L_{loc} as a function of energy from its size dependence. In Fig. 4, we plot $1/L_{\mathrm{loc}}$ against energy for several values of Δ. As Δ increases from zero, $1/L_{\mathrm{loc}}$ gradually decreases, and the value around $\varepsilon=0$ reaches almost zero (i.e., the states extended) at $\Delta \sim 0.8\Gamma$. The center value recovers to nonzero again in even larger Δ, and the peak grows rapidly as Δ increases; the states at the gap region become localized more and more.

The corresponding plots for the single-valley Hall con-

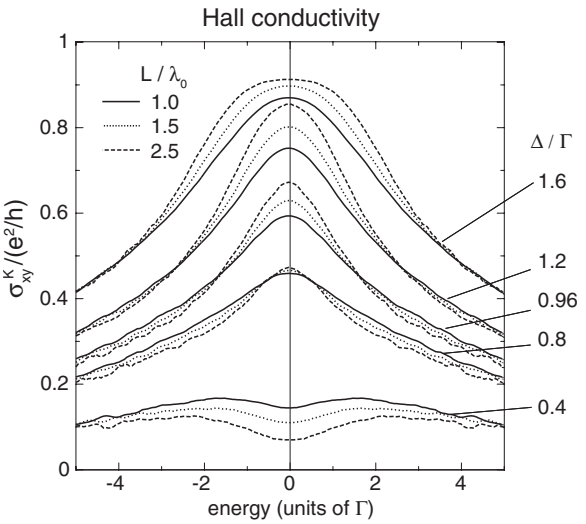

FIG. 5. Hall conductivity of a single-valley K Hamiltonian of bilayer graphene with several Δ's plotted against the energy.

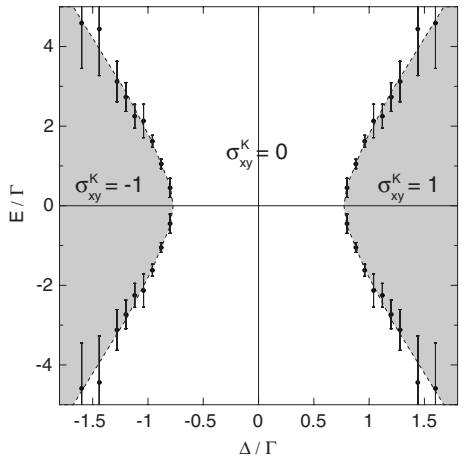

FIG. 6. Hall plateau diagram against Δ and energy E. Dots represent the critical energies estimated from the size dependence of σ_{xy}^K. Dashed curves are guides for the eyes for the phase boundary.

ductivity σ_{xy}^K are shown in Fig. 5. σ_{xy}^K becomes completely 0 at $\Delta=0$ (not shown), and the value generally goes up as Δ increases. At each single Δ, we notice that σ_{xy}^K moves in a specific direction as the system size L expands. At $\Delta=0.4\Gamma$, σ_{xy}^K decreases in all the energy as L increases. At $\Delta=1.6\Gamma$, on the contrary, σ_{xy}^K around $\varepsilon=0$ evolves in the upward direction, oppositely. The critical value of Δ where the σ_{xy}^K switches its evolving direction depends on the energy. At $E=0$, this is close to $\Delta/\Gamma=0.8$.

In the integer quantum Hall effect, the Hall conductivity in the infinite system is quantized as long as the states at the Fermi energy are localized.[27] In finite-size systems, the Hall conductivity averaged over disorder configurations generally takes noninteger values, while it gradually approaches the quantized value as the system size expands.[28] Therefore the quantized Hall conductivity in the infinite system can be estimated from the scaling behavior of finite-size values. In the above results, we expect that the region of decreasing σ_{xy}^K becomes the Hall plateau with $\sigma_{xy}^K=0$ and that of increasing σ_{xy}^K becomes the plateau with e^2/h in an infinite-system size. The point where the σ_{xy}^K switches the scaling dependence can be regarded as the phase transition between the different Hall phases $\sigma_{xy}^K=0$ and 1. Significantly this point coincides well with the divergence of the localization length L_{loc} in Fig. 4. The feature is most striking at $\Delta=0.8\Gamma$, where σ_{xy}^K at $\varepsilon=0$ is about to change its size dependence and L_{loc} at the center is also near divergence. This is a consistent result since the electronic states must be delocalized at the critical point separating different Hall plateaus.[27]

Indeed, when the energy-gap width is much larger than the disorder strength, i.e., $\Delta/\Gamma \gg 1$, we reasonably expect that σ_{xy}^K around zero energy is quantized at e^2/h, the midgap value in the clean limit, since the gap remains almost intact in the weak disorder. When the energy gap is small enough, that is, $\Delta/\Gamma \ll 1$, on the other hand, it is natural that σ_{xy}^K vanishes to zero as in the zero-gap case since the effect of Δ is completely washed out by the strong disorder. It is then inevitable to have the phase transition at the intermediate value of Δ/Γ, which is presumably of the order of 1, while the factor may depend on the specific disorder model.

At $\Delta>0.8$, we have two critical energies which separate upward and downward moving regions in σ_{xy}^K in Fig. 5. The localization length in Fig. 4 is huge around the corresponding energies, so that it becomes harder to specify the critical points out of them due to the numerical error. Figure 6 shows the phase diagram speculated in the infinite system, where each phase corresponds to the Hall plateau with quantized σ_{xy}^K. We determine the phase boundary by taking points where σ_{xy}^K changes its moving direction. The dashed curves separating the phases are guides for eyes. The phase diagram is symmetric with respect to $\Delta=0$, while the sign of the Hall conductivity is opposite between negative and positive Δ's.

We cannot eliminate the delocalized states as long as K and K' valleys are decoupled in the following sense: In the clean system, as previously discussed, the single-valley Hall conductivity σ_{xy}^K at the gap is quantized at -1 and 1 (in units of e^2/h) at negative and positive Δ, respectively. In the disordered system, we expect that σ_{xy}^K at the gap remains quantized when the gap width is large enough compared to the energy broadening due to the disorder. Thus the Hall conductivity at a fixed Fermi energy definitely changes from -1 to 1 when Δ changes from $-\Delta_0$ to $+\Delta_0$ with sufficiently large Δ_0. This requires that the delocalized states appear at that energy somewhere between $-\Delta_0$ and $+\Delta_0$ because otherwise the Hall conductivity stays constant.[27] The present calculation indeed suggests that there are two delocalized points of Δ (negative and positive) at each fixed energy.

The delocalized states would disappear in presence of the short-ranged disorder with atomic length scale, which induces intervalley coupling between K and K' and makes the original time-reversal symmetry effective. The localization length at the phase boundary is expected to diverge as the intervalley scattering rate goes to zero. The trigonal warping effect due to the extra hopping parameter, which is also neglected here, does not kill the delocalized states since it does not mix the valleys, while it generally weakens the electron localization at $\Delta=0$.[16]

In this paper we proposed that the external electric field applied to the bilayer graphene causes a phase transition at which the localization length diverges. The transition can be interpreted as an analog of quantum Hall transition at each single valley. While the actual Hall conductivity is never directly observed, it may be possible to observe the divergence of the localization length in a temperature (T) dependence of the conductivity σ_{xx} as in the conventional integer quantum Hall effect.[29] Figure 3(b) can be approximately viewed as plots of σ_{xx} at different T's when we use a relation $\sigma_{xx} \sim (e^2/\hbar)g$ and regard L as the phase-coherent length at T. When the system goes through the phase transition, σ_{xx} exhibits a peak at the phase boundary and its peak width becomes narrower as the temperature is lowered.[29] To observe this, the temperature must be low enough that the phase-coherent length exceeds the typical localization length l_B. Our calculation is based on a typical disorder model used in theories, while it may not describe some specific situations in the real bilayer graphene currently available, which is supposed to include puddles (long-range inhomogeneity) or impurity-bound states described by the variable-range hopping model. We leave to the future work the study on those effects on the present phenomenon.

The author acknowledges helpful interactions with K. Nomura, S. Ryu, B. Altshuler, I. L. Aleiner, B. Özyilmaz, and P. Kim. This work was supported in part by the 21st Century COE Program at Tokyo Tech "Nanometer-Scale Quantum Physics" and by Grants-in-Aid for Scientific Research from the Ministry of Education, Culture, Sports, Science and Technology, Japan.

[1] K. S. Novoselov, A. K. Geim, S. V. Morozov, D. Jiang, Y. Zhang, S. V. Dubonos, I. V. Grigorieva, and A. A. Firsov, Science **306**, 666 (2004).
[2] K. S. Novoselov, A. K. Geim, S. V. Morozov, D. Jiang, M. I. Katsnelson, I. V. Grigorieva, S. V. Dubonos, and A. A. Firsov, Nature (London) **438**, 197 (2005).
[3] Y. Zhang, Y. W. Tan, H. L. Stormer, and P. Kim, Nature (London) **438**, 201 (2005).
[4] K. S. Novoselov, E. McCann, S. V. Morozov, V. I. Fal'ko, M. I. Katsnelson, U. Zeitler, D. Jiang, F. Schedin, and A. K. Geim, Nat. Phys. **2**, 177 (2006).
[5] T. Ohta, A. Bostwick, T. Seyller, K. Horn, and E. Rotenberg, Science **313**, 951 (2006).
[6] E. McCann and V. I. Fal'ko, Phys. Rev. Lett. **96**, 086805 (2006).
[7] R. V. Gorbachev, F. V. Tikhonenko, A. S. Mayorov, D. W. Horsell, and A. K. Savchenko, Phys. Rev. Lett. **98**, 176805 (2007).
[8] S. V. Morozov, K. S. Novoselov, M. I. Katsnelson, F. Schedin, D. Elias, J. A. Jaszczak, and A. K. Geim, Phys. Rev. Lett. **100**, 016602 (2008).
[9] M. Koshino and T. Ando, Phys. Rev. B **73**, 245403 (2006).
[10] M. I. Katsnelson, Eur. Phys. J. B **52**, 151 (2006).
[11] I. Snyman and C. W. J. Beenakker, Phys. Rev. B **75**, 045322 (2007).
[12] J. Cserti, Phys. Rev. B **75**, 033405 (2007).
[13] J. Cserti, A. Csordas, and G. David, Phys. Rev. Lett. **99**, 066802 (2007).
[14] H. Suzuura and T. Ando, Phys. Rev. Lett. **89**, 266603 (2002); E. McCann, K. Kechedzhi, V. I. Falko, H. Suzuura, T. Ando, and B. L. Altshuler, *ibid.* **97**, 146805 (2006); I. L. Aleiner and K. B. Efetov, *ibid.* **97**, 236801 (2006); A. Altland, *ibid.* **97**, 236802 (2006); K. Nomura, M. Koshino, and S. Ryu, *ibid.* **99**, 146806 (2007).
[15] S. V. Morozov, K. S. Novoselov, M. I. Katsnelson, F. Schedin, L. A. Ponomarenko, D. Jiang, and A. K. Geim, Phys. Rev. Lett. **97**, 016801 (2006); X. Wu, X. Li, Z. Song, C. Berger, and W. A. de Heer, *ibid.* **98**, 136801 (2007); H. B. Heersche, P. Jarillo-Herrero, J. B. Oostinga, L. M. K. Vandersypen, and A. F. Morpurgo, Nature (London) **446**, 56 (2007).
[16] K. Kechedzhi, V. I. Fal'ko, E. McCann, and B. L. Altshuler, Phys. Rev. Lett. **98**, 176806 (2007).
[17] E. McCann, Phys. Rev. B **74**, 161403(R) (2006).
[18] E. V. Castro, K. S. Novoselov, S. V. Morozov, N. M. R. Peres, J. M. B. Lopes dos Santos, J. Nilsson, F. Guinea, A. K. Geim, and A. H. Castro Neto, Phys. Rev. Lett. **99**, 216802 (2007).
[19] Hongki Min, Bhagawan Sahu, Sanjay K. Banerjee, and A. H. MacDonald, Phys. Rev. B **75**, 155115 (2007).
[20] J. Nilsson and A. H. Castro Neto, Phys. Rev. Lett. **98**, 126801 (2007).
[21] J. Nilsson, A. H. Castro Neto, F. Guinea, and N. M. R. Peres, Phys. Rev. B **76**, 165416 (2007).
[22] J. B. Oostinga, H. B. Heersche, X. Liu, A. F. Morpurgo, and L. M. K. Vandersypen, Nature Mater. **7**, 151 (2008).
[23] G. W. Semenoff, Phys. Rev. Lett. **53**, 2449 (1984).
[24] A. W. W. Ludwig, M. P. A. Fisher, R. Shankar, and G. Grinstein, Phys. Rev. B **50**, 7526 (1994).
[25] G. Giovannetti, P. A. Khomyakov, G. Brocks, P. J. Kelly, and J. van den Brink, Phys. Rev. B **76**, 073103 (2007).
[26] Y. Imry, *Introduction to Mesoscopic Physics* (Oxford University Press, Oxford, 1997), and references therein.
[27] A. M. M. Pruisken, in *The Quantum Hall Effect*, edited by R. E. Prange and S. M. Girvin (Springer-Verlag, Berlin, 1990).
[28] T. Ando, J. Phys. Soc. Jpn. **55**, 3199 (1986).
[29] H. P. Wei, D. C. Tsui, M. A. Paalanen, and A. M. M. Pruisken, Phys. Rev. Lett. **61**, 1294 (1988).